Metal–Organic Frameworks

International Edition: DOI: 10.1002/anie.201504758
German Edition: DOI: 10.1002/ange.201504758

Metal–Organic Frameworks (MOFs) of a Cubic Metal Cluster with Multicentered Mn^I–Mn^I Bonds

Huan-Cheng Hu, Han-Shi Hu, Bin Zhao, Ping Cui, Peng Cheng, and Jun Li**

Abstract: *MOFs with both multicentered metal–metal bonds and low-oxidation-state (LOS) metal ions have been underexplored hitherto. Here we report the first cubic [Mn^I_8] cluster-based MOF (**1**) with multicentered Mn^I–Mn^I bonds and +1 oxidation state of manganese (Mn^I or Mn(I)), as is supported by single-crystal structure determination, XPS analyses, and quantum chemical studies. Compound **1** possesses the shortest Mn^I–Mn^I bond of 2.372 Å. Theoretical studies with density functional theory (DFT) reveal extensive electron delocalization over the [Mn^I_8] cube. The 48 electrons in the [Mn^I_8] cube fully occupy half of the 3d-based and the lowest 4s-based bonding orbitals, with six electrons lying at the nonbonding 3d-orbitals. This bonding feature renders so-called cubic aromaticity. Magnetic properties measurements show that **1** is an antiferromagnet. This work is expected to inspire further investigation of cubic metal–metal bonding, MOF materials with LOS metals, and metalloaromatic theory.*

In the past two decades, metal–organic frameworks (MOFs) have attracted much attention due to their fascinating topological structures and various functions in adsorption, separation, catalysis, chemical sensing, and magnetic properties.[1,2] In construction and design of MOFs with characteristic properties and functions, metal ions play a crucial role. Especially, through small bridging molecules metal ions can be aggregated into more complicated cages/clusters, which serve as nodes and can form highly connected MOFs.[3] In more than 25000 MOF-related publications, cluster-based MOFs with low-oxidation-state (LOS) metals and multicentered metal–metal bonding were unknown until recently when a Zn_8 cluster was synthesized.[4]

On the other hand, oxidation state as a central concept in chemistry is associated with both the electronic structure and chemical properties of a given atom. Among all the elements in the periodic table, the lowest oxidation state is −4 for carbon,[5a] and the highest oxidation state is +9 for iridium.[5b] Due to their low electronegativity, metals tend to have high oxidation states, whereas LOS of metals are rare and often offer opportunity for unique electronic structures and properties. Recently, the number of LOS metal–metal bonded compounds have rapidly increased since Carmona's report of the singly bonded zinc(I) dimer [Cp*ZnZnCp*] (Cp* = C_5Me_5).[6] A number of M^I–M^I bonded compounds have been synthesized, including M = Cd,[7,12d] Cr,[8] In,[9] Mg,[10] Fe,[11,12e] Mn,[12] Co,[13] and Ni.[14] These compounds all contained dinuclear metals (except In) and were obtained by using sterically demanding ligands. Most of them are unstable in air. So far multicentered Mn^I–Mn^I bonded polyatomic clusters have not yet been reported, although dinuclear Mn^I–Mn^I bonded compounds are known.[12]

In this work, we report the synthesis of the first polyatomic Mn^I compound $\{[Mn^I_8Mn^{II}_3(H_2O)_6(HL)_{12}](OH)_2\cdot 17H_2O\}_n$ (**1**) (L = tetrazole dianion), which features +1 oxidation state, multicenter Mn^I–Mn^I bonding, and the shortest Mn^I–Mn^I distance. The chemical stability, magnetic properties, electronic structure, and bonding character are also investigated.

Air- and moisture-stable crystals of **1** were prepared by in situ [2+3] cycloaddition reaction of NaN_3, $KC(CN)_3$, and $MnCl_2$ in a mixture of H_2O and EtOH (v/v = 4:1) at 145 °C for 72 h. Single-crystal X-ray diffraction (SCXRD) analyses reveal that **1** crystallizes in the cubic system with space group *Pm3m*. Two crystallographically independent Mn centers exist in each asymmetric unit (Figure 1 and Figure S1 in the Supporting Information, SI). Mn1 is located on a three-fold axis with Wyckoff notation *g* and point symmetry 3*m*, and Mn2 stands on the intersection of a four-fold axis and mirror plane with Wyckoff notation *c* and point symmetry 4/*mmm*. Mn1 atom is bonded with three N atoms (N1, N1A, and N1B) from three HL^- monoanion ligands with Mn1–N1 bond length of 2.177 Å, and three adjacent equivalent Mn1 atoms. The distorted octahedral coordination geometry of Mn2 is finished by four N atoms (N3, N3A, N3B, and N3C) with Mn2–N3 = 2.259 Å and two water molecules (O1 and O1A) with Mn2–O1 = 2.060 Å.

The eight equivalent Mn1 atoms as the vertex are found to form a perfect cube [Mn^I_8] with O_h symmetry from SCXRD characterization. Surprisingly, the twelve Mn^I–Mn^I distances are completely identical and the bond (2.372 Å) is shorter than the sum of covalent radii for Mn^I (2.480 Å),[15] indicative of the existence of direct Mn^I–Mn^I bonding. This Mn–Mn distance is significantly shorter than all reported Mn^I–Mn^I bonds, 2.636 Å in $Mn_4S_2(CO)_{15}(PMe_2Ph)_2$, 2.674 Å in $Mn_2(CO)_7(\mu\text{-}S_2)$, 2.717 Å in $[Mn^I_2(\mu\text{-}N,N'\text{-Pipiso})_2]$ (Pipiso = $(DipN)_2C(cis\text{-}2,6\text{-}Me_2NC_5H_8)$), 2.721 Å in [{HC-

[*] H.-C. Hu,[+] Prof. Dr. B. Zhao, P. Cui, Prof. Dr. P. Cheng
Department of Chemistry, Key Laboratory of Advanced Energy Material Chemistry, Nankai University and Collaborative Innovation Center of Chemical Science and Engineering (Tianjin)
Tianjin 300071 (China)
E-mail: zhaobin@nankai.edu.cn
H.-S. Hu,[+] Prof. Dr. J. Li
Department of Chemistry, Key Laboratory of Organic Optoelectronics and Molecular Engineering of Ministry of Education, Tsinghua University
Beijing 100084 (China)
E-mail: junli@tsinghua.edu.cn
[+] These authors contributed equally to this work.

Supporting information for this article is available on the WWW under http://dx.doi.org/10.1002/anie.201504758.

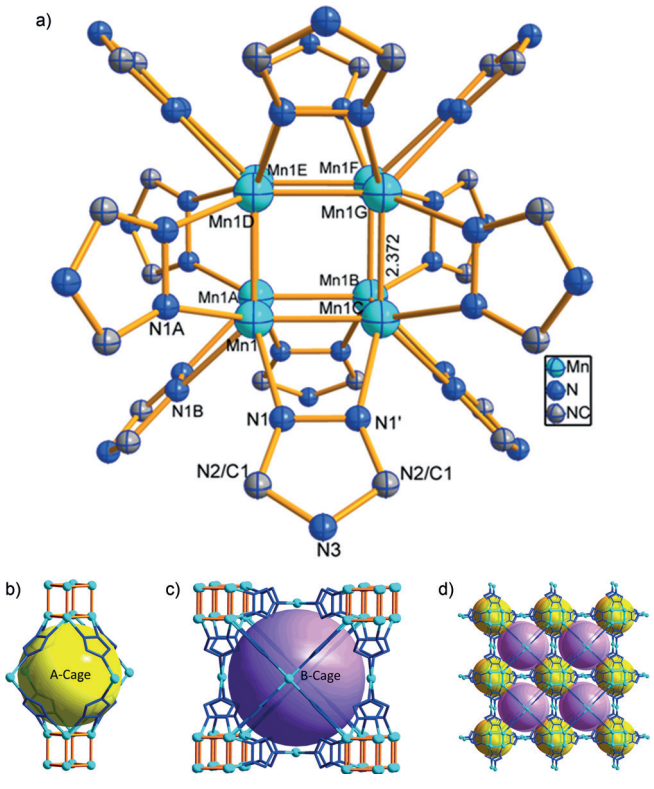

Figure 1. a) The Mn^{I}–Mn^{I} bonded $[Mn^{I}_{8}]$ cube with O_h symmetry in **1**. b) and c) Two types of cages (yellow: A-cage, pink: B-cage). d) 3D framework consisting of two types of cages along the *c*-axis. O atoms omitted for clarity.

$(CMeNAr)_2\}Mn]_2$, and 2.787 Å in $[(thf)_2K\subset 18\text{-crown-}6]_2[Mn\{\kappa^2\text{-}Me_2Si(NDipp)_2\}_2]$ (Dipp = 2,6-$iPr_2C_6H_3$).[12] It is in fact the shortest Mn^{I}–Mn^{I} bond observed so far. Compared with the distorted Zn^{I}_{8} cubes with low symmetry of D_{4h} and D_{2d},[4] it is the first time to obtain an M^{I}–M^{I} bonded cube with perfect O_h high symmetry.

In the crystal structure, one $[Mn^{I}_{8}]$ cube is supported by twelve tetrazole rings (Figure 1 a), and one tetrazole ring coordinates to only one Mn2 atom. As a result, each $[Mn^{I}_{8}]$ cube is surrounded by 12 adjacent Mn2 atoms and each Mn2 atom links to four adjacent $[Mn^{I}_{8}]$ cubes. The $[Mn^{I}_{8}]$ cube and Mn2 can be simplified as 12-connected and 4-connected node, respectively (Figure S1), which gives rise to a (12, 4) high-connection 3D framework with **ftw** topology and the point symbol $\{4^{36}.6^{30}\}\{4^4.6^2\}_3$. To our knowledge, **ftw** topology with different metal centers as nodes is not frequently observed in MOFs.[16] A- and B-cage with diameters of 8.0 and 10.5 Å exist in the 3D framework (Figure 1 b and c), respectively. The A-cage is formed by four Mn2 atoms and two $[Mn^{I}_{8}]$ cubes, whereas the B-cage is constructed by six nearby Mn2 atoms and eight $[Mn^{I}_{8}]$ cubes. Twelve A-cages surround one B-cage, whereas four B-cages embrace one A-cage. Thus, the overall network consists of two types of cages with the stacking ratio of 3:1 (Figure 1 d). Additionally, after the removal of guest molecules, the void volume of **1** is 37.5 % by using the PLATON software.[17] However, owing to the very low N_2 gas absorption capacity at 77 K, the surface area of **1** was not experimentally determined (Figure S2).

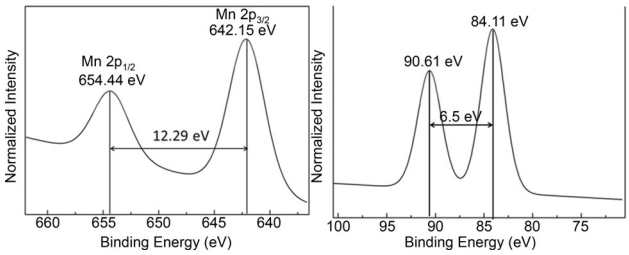

Figure 2. XPS spectra of Mn in compound **1**, Mn 2p (left) and Mn 3s (right).

X-ray photoelectron spectra (XPS) of **1** were measured to explore the oxidation state of manganese. Typical Mn-2p and Mn-3s spectra were obtained (Figure 2). The binding energies of Mn-$2p_{3/2}$ and Mn-$2p_{1/2}$ are 642.15 and 654.44 eV, respectively, and their energy gap of 12.29 eV clearly deviates from the corresponding value of 11.8 eV in Mn^{II} compounds. Furthermore, due to the parallel spin coupling between 3s electrons and unpaired 3d electrons during the photoelectron ejection,[18a,b] the Mn-3s spectra exhibit two peaks at 84.11 and 90.61 eV with the energy separation of 6.5 eV. Theoretically, the splitting of Mn-3s binding energy (ΔE_{3s}) strongly depends on the oxidation states of Mn ions, with larger ΔE_{3s} for lower oxidation states.[18] The ΔE_{3s} of Mn^{II}, Mn^{III}, and Mn^{IV} is 6.1 eV,[19a,b] 5.4 eV,[18b,19c] and 4.8 eV,[19d] respectively. There exists a linear relationship between ΔE_{3s} and oxidation states of Mn ions as shown in Figure S3, in which the predicted ΔE_{3s} of Mn^{I} is about 6.7 eV. The measured ΔE_{3s} of 6.5 eV in **1** is close to this value, and is much larger than the reported value of Mn^{II}, indicating unambiguously that Mn centers in **1** exhibit a lower oxidation state than +2. Furthermore, the slight deviation of the experimental value (6.5 eV) from the expected 6.7 eV of Mn^{I} is likely due to the perturbation of Mn^{II} in **1**, supporting the existence of the +1 oxidation state Mn. Interestingly, although the 3D framework of **1** differs largely from that in the $[Zn^{I}_{8}]$ compound, the $[Mn^{I}_{8}]$ cube as a building block in **1** is similar to the $[Zn^{I}_{8}]$ cube.[4]

To elucidate the chemical bonding and electronic structure of the cluster in **1**, DFT calculations were carried out on the $[Mn^{I}_{8}]^{8+}$ core and $[Mn_8(HL)_{12}]^n$ ($n = 4-, 1-, 2+$, and $4+$) clusters with various oxidation states of Mn. The computational methods and results are described in the SI. Our calculations show that the $[Mn_8(HL)_{12}]^{4-}$ cluster with Mn^{I} has Mn–Mn bonds of 2.37 Å, which is consistent with the measured value (Table S1, SI). The energy levels of the frontier 4s- and 3d-bands formed by eight $Mn^{I}(4s^13d^5)$ atoms in $[Mn_8(HL)_{12}]^{4-}$ with O_h symmetry are shown in Figure 3, with the isosurfaces of the 3d- and 4s-based MOs of the $[Mn^{I}_{8}]$ cube shown in Tables S2 and S3. Interestingly, the 3d-band spans energetically only about 1/3 of the 4s-band due to much contracted Mn 3d shell. The 4s- and $3d_{z^2}$-based MOs form two sets of bonding MOs with a_{1g} and t_{1u} symmetries and antibonding MOs with t_{2g} and a_{2u} symmetries, respectively (Table S3). The occupation of the a_{1g} orbital of the 4s-band and the $a_{1g} + t_{1u}$ of the 3d-band, leads to dual cubic aromaticity in the $[Mn^{I}_{8}]$ cube (Figure 4), instead of eight electrons in the 4s-based cubic aromaticity in $[Zn^{I}_{8}]$ with Zn^{I} ($4s^13d^{10}$) atoms.[4] Consequently, the 4s-electrons obey the cubic aromaticity

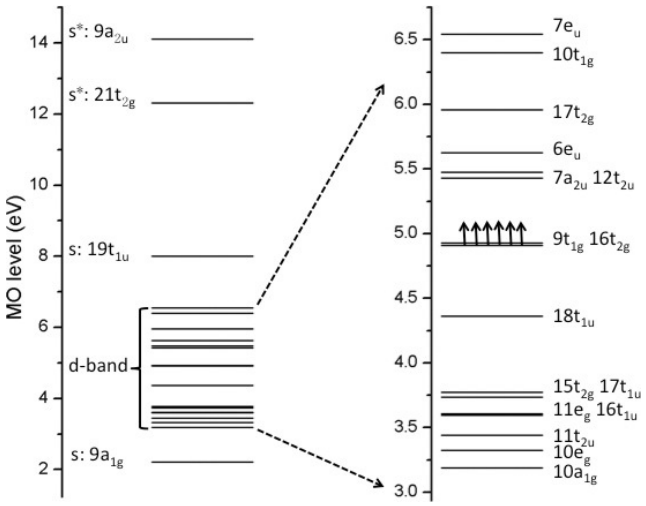

Figure 3. The energy levels of $[Mn_8(HL)_{12}]^{4-}$. Left, the frontier molecular orbital energy levels including s- and d-bands; inset at right, the enlarged d-band levels.

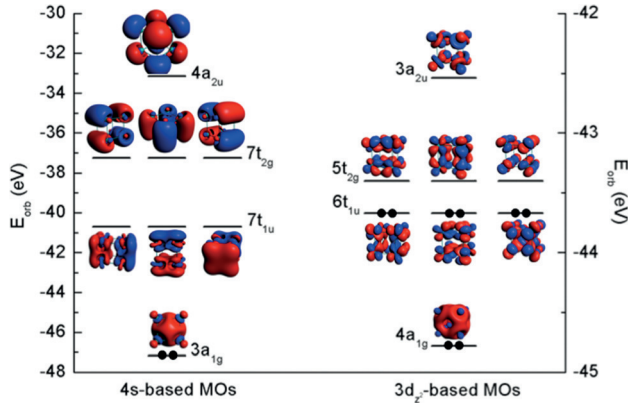

Figure 4. The bonding pattern in the $[Mn^{I}_8]$ cube with dual cubic aromaticity from 4s-based and $3d_{z^2}$-based molecular orbitals, respectively.

rule of $6n+2$ at $n=0$, and the $3d_{z^2}$-electrons obey the rule of $6n+2$ at $n=1$. All bonding MOs of the 3d-band are fully occupied, except for the frontier six electrons that are occupying the almost degenerate nonbonding 3d-based $9t_{1g}$ and $16t_{2g}$ orbitals, leading to possible magnetism (right part of Figure 3) in the d-band, due to their lower energy levels than those of the 4s-based $19t_{1u}$ orbital. In other words, the forty electrons from eight $Mn^{I}(3d^5)$ are maintained in the lowest twenty orbitals of the d-band, together with the two electrons on the $9a_{1g}$ orbital of the s-band, accounting for the multicenter bonding of the $[Mn^{I}_8]$ cube. This rare dual cubic aromaticity partly explains the shortest Mn–Mn bond and high thermal stability of **1**. The oxidation state of Mn2 in **1** is +2 based on the empirical bond-valence calculation (Table S5).[20]

To experimentally probe the chemical stability, compound **1** was immersed in common solvents, including H_2O, MeOH, EtOH, DMF, CCl_4, cyclohexane, *n*-hexane, and MeCN for 24 h. The resulting sample still retains crystalline state, and the corresponding experimental powder X-ray diffraction (PXRD) patterns agree well with the simulated from the single-crystal structure data (Figure S4), indicating superb chemical stability of **1** in these solvents. Additionally, thermogravimetric analysis (TGA) revealed that the 3D framework in **1** starts to collapse at about 360 °C (Figure S5), indirectly confirming the high thermal stability of the $[Mn^{I}_8]$ cubic clusters in frameworks.

The temperature dependence of the magnetic susceptibility of compound **1** was measured under 1000 Oe in the temperature range of 1.8–300 K (Figure S6), the room-temperature χT value measured at 33.96 $cm^3 K mol^{-1}$ is much smaller than the expected spin-only value of 61.12 $cm^3 K mol^{-1}$ for eight Mn^{I} and three Mn^{II} ions ($3d^54s^1$ for Mn^{I}, and $3d^5$ for Mn^{II} ions) with $g=2.0$, similar to the reported manganese(I) dimer.[12c–e] The large divergence implies metal–metal bonding in the $[Mn^{I}_8]$ cube that decreases the number of unpaired 3d or 4s electrons in the $[Mn^{I}_8]$ cube. Upon lowering temperature, the value of χT is reduced gradually to 3.82 $cm^3 K mol^{-1}$ at 1.8 K, indicative of the antiferromagnetic coupling amongst Mn ions. The curve of χ^{-1} versus T above 4 K obeys the Curie–Weiss law with the Curie constant $C=36.94$ $cm^3 K mol^{-1}$ and the Weiss constant $\theta=-25.74$ K. The negative Weiss constant further supports the presence of dominant antiferromagnetic interactions in **1**. Additionally, the χ_M value exhibits a rapid increase with the decreasing temperature and reaches its maximum at 2.2 K, and then decreases with further cooling (Figure S7). The magnetic behavior implies that 3D long-range antiferromagnetic ordering exists in **1** with the Neèl temperature T_N of about 2.2 K.[21]

To further determine the critical temperature of 3D magnetic ordering, the temperature dependences of field-cooled (FC) and zero-field-cooled (ZFC) magnetization at 50 Oe were measured (Figure 5). The peaks occur at 2.2 K in FC and ZFC curves, revealing the occurrence of an antiferromagnetic ordering at 2.2 K. Additionally, alternate current (AC) magnetic susceptibility at zero DC field and 3 Oe oscillating field with different frequencies were measured. In the χ' (in-phase component in AC susceptibility)

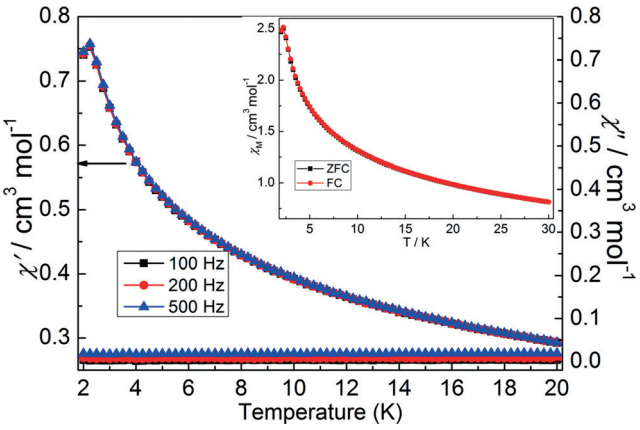

Figure 5. The plots of in-phase (χ') and out-of-phase (χ'') AC susceptibility versus temperature under 3 Oe oscillating field and different frequencies. Inset: Plots of FC and ZFC for **1** using a field of 50 Oe.

versus T plot, the frequency-independent peaks are clearly observed at 2.2 K, whereas no peaks appear in the χ'' (out-of-phase component in AC susceptibility) versus T plot. The frequency-independent behavior in AC susceptibility precludes the presence of slow magnetic relaxation and spin-glass behavior,[22] and indicates that **1** is an antiferromagnet below 2.2 K.

The magnetization isotherm of **1** was measured at 1.8 K in fields of 0–8 T. The magnetization values increase very rapidly and almost linearly with the increasing field. However, it does not saturate and the maximum value of magnetization is 15.3 Nβ at 8 T, which is far below the saturation value (63.0 Nβ) expected for isolated eight Mn^{I} and three Mn^{II} species. This behavior is indicative of the formation of Mn^{I}–Mn^{I} bonds and antiferromagnetic coupling within **1**. Meanwhile, a small hysteresis loop (Figure S8) with the coercive field $H_C = 30$ Oe and remnant magnetization $M_r = 0.0184$ Nβ was detected at 1.8 K, demonstrating the feature of a soft magnet.

To determine the critical field from antiferromagnet to paramagnet for **1**, the temperature-dependent AC susceptibilities under the frequency of 200 Hz and different external magnetic fields from 100 to 1900 Oe were measured (Figure S9). The peak of χ' versus T gradually shifts from 2.2 K to lower temperature with increasing external magnetic fields, and it disappears when the applied magnetic field reaches 500 Oe, implying that the antiferromagnetic long-range ordering in **1** can be destroyed under the external magnetic field above 500 Oe.

In summary, a $[Mn^{I}_{8}]$ cubic-cluster-based metal–organic framework has been synthesized and structurally characterized to possess multicentered Mn^{I}–Mn^{I} bonds and the shortest Mn^{I}–Mn^{I} distance. This MOF material displays high thermal and chemical stability. Theoretical studies show that there are 42 electrons contributing to the multicenter bonding of the $[Mn^{I}_{8}]$ cube and six electrons that may contribute to its magnetic property. Magnetic investigations suggest that the antiferromagnetic long-range ordering in **1** occurs at about 2.2 K, and the critical field from antiferromagnet to paramagnet was determined at approximately 500 Oe. This work might provide insights for constructing novel MOF materials with M^{I}–M^{I} bonds, and adds new examples of metal clusters with multicentered metal–metal bonding and cubic aromaticity.

Experimental Section

Synthesis of **1**: $MnCl_2{\cdot}4H_2O$ (0.3 mmol, 0.0591 g), NaN_3 (0.6 mmol, 0.39 g), and $KC(CN)_3$ (0.1 mmol, 0.0129 g) were dissolved in H_2O and EtOH (10 mL, v/v 4:1) mixed solvents in a 25 mL Teflon-lined stainless vessel. The vessel was heated in a 145 °C oven for 72 h, and then slowly cooled down to room temperature at 2 °C h^{-1}. Colorless cubic crystals were obtained by filtration and the yield of **1** was 52 % (based on $MnCl_2{\cdot}4H_2O$). Anal. Calcd. (%) for $C_{12}H_{60}Mn_{11}N_{48}O_{25}$: C, 7.66; H, 3.21; N, 35.74; Found: C, 7.82; H, 2.99; N, 35.60. Selected IR (KBr, cm^{-1}): 3438(sb), 1638 (vs), 1451 (w), 1415 (m), 1157 (m), 1130 (m), 1047 (s), 944 (s), 758 (m), 618 (wb). UV/Vis spectra and crystal data from single-crystal diffraction studies for **1** is given in SI.

Acknowledgements

This project was financially supported by the 973 Program (2012CB821702, 2011CB932401, and 2011CB935902), NSFC (21421001 and 21473121), SFC of Tianjin (15JCZDJC37700), 111 project (B12015), and MOE Innovation Team (IRT13022 and IRT-13R30) of China.

Keywords: antiferromagnets · cubic aromaticity · metal clusters · metal–organic frameworks · multicenter Mn^{I}–Mn^{I} bonds

How to cite: *Angew. Chem. Int. Ed.* **2015**, *54*, 11681–11685
Angew. Chem. **2015**, *127*, 11847–11851

[1] a) X. Zhao, X. H. Bu, Q. G. Zhai, H. Tran, P. Y. Feng, *J. Am. Chem. Soc.* **2015**, *137*, 1396–1399; b) W. Y. Gao, Y. Chen, Y. H. Niu, K. Williams, L. Cash, P. J. Perez, L. Wojtas, J. F. Cai, Y. S. Chen, S. Q. Ma, *Angew. Chem. Int. Ed.* **2014**, *53*, 2615–2619; *Angew. Chem.* **2014**, *126*, 2653–2657; c) D. W. Feng, K. C. Wang, Z. W. Wei, Y. P. Chen, C. M. Simon, R. K. Arvapally, R. L. Martin, M. Bosch, T. F. Liu, S. Fordham, D. Q. Yuan, M. A. Omary, M. Haranczyk, B. Smit, H. C. Zhou, *Nat. Commun.* **2014**, *5*, 5723; d) N. T. T. Nguyen, H. Furukawa, F. Gándara, H. T. Nguyen, K. E. Cordova, O. M. Yaghi, *Angew. Chem. Int. Ed.* **2014**, *53*, 10645–10648; *Angew. Chem.* **2014**, *126*, 10821–10824; e) C. Y. Sun, X. L. Wang, X. Zhang, C. Qin, P. Li, Z. M. Su, D. X. Zhu, G. G. Shan, K. Z. Shao, J. Li, *Nat. Commun.* **2013**, *4*, 2717; f) D. J. Xiao, E. D. Bloch, J. A. Mason, W. L. Queen, M. R. Hudson, N. Planas, J. Borycz, A. L. Dzubak, P. Verma, K. Lee, F. Bonino, V. Crocellà, J. Yano, S. Bordiga, D. G. Truhlar, L. Gagliardi, C. M. Brown, J. R. Long, *Nat. Chem.* **2014**, *6*, 590–595; g) C. B. He, K. D. Lu, W. B. Lin, *J. Am. Chem. Soc.* **2014**, *136*, 12253–12256; h) H. H. Fei, J. W. Shin, Y. S. Meng, M. Adelhardt, J. Sutter, K. Meyer, S. M. Cohen, *J. Am. Chem. Soc.* **2014**, *136*, 4965–4973; i) J. C. Yu, Y. J. Cui, Y. Yang, Z. Y. Wang, B. L. Chen, G. D. Qian, *Nat. Commun.* **2013**, *4*, 2719; j) S. K. Elsaidi, M. H. Mohamed, L. Wojtas, A. Chanthapally, T. Pham, B. Space, J. J. Vittal, M. J. Zaworotko, *J. Am. Chem. Soc.* **2014**, *136*, 5072–5077.

[2] a) H. C. Zhou, S. Kitagawa, *Chem. Soc. Rev.* **2014**, *43*, 5415–5418; b) Z. C. Hu, B. J. Deibert, J. Li, *Chem. Soc. Rev.* **2014**, *43*, 5815–5840; c) E. Coronado, G. M. Espallargas, *Chem. Soc. Rev.* **2013**, *42*, 1525–1539; d) P. Cui, Y. G. Ma, H. H. Li, B. Zhao, J. R. Li, P. Cheng, P. B. Balbuena, H. C. Zhou, *J. Am. Chem. Soc.* **2012**, *134*, 18892–18895.

[3] a) X. F. Kuang, X. Y. Wu, R. M. Yu, J. P. Donahue, J. S. Huang, C. Z. Lu, *Nat. Chem.* **2010**, *2*, 461–465; b) V. Guillerm, Ł. J. Weseliński, Y. Belmabkhout, A. J. Cairns, V. D'Elia, Ł. Wojtas, K. Adil, M. Eddaoudi, *Nat. Chem.* **2014**, *6*, 673–680; c) J. F. Eubank, F. Nouar, R. Luebke, A. J. Cairns, L. Wojtas, M. Alkordi, T. Bousquet, M. R. Hight, J. Eckert, J. P. Embs, P. A. Georgiev, M. Eddaoudi, *Angew. Chem. Int. Ed.* **2012**, *51*, 10099–10103; *Angew. Chem.* **2012**, *124*, 10246–10250; d) A. J. Cairns, J. A. Perman, L. Wojtas, V. C. Kravtsov, M. H. Alkordi, M. Eddaoudi, M. J. Zaworotko, *J. Am. Chem. Soc.* **2008**, *130*, 1560–1561.

[4] P. Cui, H. S. Hu, B. Zhao, J. T. Miller, P. Cheng, J. Li, *Nat. Commun.* **2015**, *6*, 6331.

[5] a) I. Langmuir, *J. Franklin Inst.* **1919**, *187*, 359; b) I. Langmuir, *J. Am. Chem. Soc.* **1919**, *41*, 1543–1559; c) I. Langmuir, *Proc. Nat. Acad. Sci.* **1919**, *5*, 252–259; d) G. J. Wang, M. F. Zhou, J. T. Goettel, G. J. Schrobilgen, J. Su, J. Li, T. Schlöder, S. Riedel, *Nature* **2014**, *514*, 475–477.

[6] a) I. Resa, E. Carmona, E. Gutierrez-Puebla, A. Monge, *Science* **2004**, *305*, 1136 – 1138; b) Y. Z. Wang, B. Quillian, P. R. Wei, H. Y. Wang, X. J. Yang, Y. M. Xie, R. B. King, P. von R. Schleyer, H. F. Schaefer, G. H. Robinson, *J. Am. Chem. Soc.* **2005**, *127*, 11944 – 11945; c) Z. L. Zhu, M. Brynda, R. J. Wright, R. C. Fischer, W. A. Merrill, E. Rivard, R. Wolf, J. C. Fettinger, M. M. Olmstead, P. P. Power, *J. Am. Chem. Soc.* **2007**, *129*, 10847 – 10857; d) I. L. Fedushkin, A. A. Skatova, S. Y. Ketkov, O. V. Eremenko, A. V. Piskunov, G. K. Fukin, *Angew. Chem. Int. Ed.* **2007**, *46*, 4302 – 4305; *Angew. Chem.* **2007**, *119*, 4380 – 4383; e) Y. C. Tsai, D. Y. Lu, Y. M. Lin, J. K. Hwang, J. S. K. Yu, *Chem. Commun.* **2007**, 4125 – 4127; f) T. Bollermann, K. Freitag, C. Gemel, R. W. Seidel, M. v. Hopffgarten, G. Frenking, R. A. Fischer, *Angew. Chem. Int. Ed.* **2011**, *50*, 772 – 776; *Angew. Chem.* **2011**, *123*, 798 – 802; g) D. Schuchmann, U. Westphal, S. Schulz, U. Flörke, D. Bläser, R. Boese, *Angew. Chem. Int. Ed.* **2009**, *48*, 807 – 810; *Angew. Chem.* **2009**, *121*, 821 – 824; h) S. Schulz, *Chem. Eur. J.* **2010**, *16*, 6416 – 6428; i) X. J. Yang, J. Yu, Y. Y. Liu, Y. M. Xie, H. F. Schaefer, Y. M. Liang, B. Wu, *Chem. Commun.* **2007**, 2363 – 2365; j) T. S. Li, S. Schulz, P. W. Roesky, *Chem. Soc. Rev.* **2012**, *41*, 3759 – 3771.

[7] D. L. Reger, S. S. Mason, A. L. Rheingold, *J. Am. Chem. Soc.* **1993**, *115*, 10406 – 10407.

[8] a) T. Nguyen, A. D. Sutton, M. Brynda, J. C. Fettinger, G. J. Long, P. P. Power, *Science* **2005**, *310*, 844 – 847; b) J. M. Shen, G. P. A. Yap, K. H. Theopold, *Chem. Commun.* **2014**, *50*, 2579 – 2581.

[9] M. S. Hill, P. B. Hitchcock, R. Pongtavornpinyo, *Science* **2006**, *311*, 1904 – 1907.

[10] a) S. P. Green, C. Jones, A. Stasch, *Science* **2007**, *318*, 1754 – 1757; b) A. Stasch, C. Jones, *Dalton Trans.* **2011**, *40*, 5659 – 5672.

[11] T. Nguyen, W. A. Merrill, C. Ni, H. Lei, J. C. Fettinger, B. D. Ellis, G. J. Long, M. Brynda, P. P. Power, *Angew. Chem. Int. Ed.* **2008**, *47*, 9115 – 9117; *Angew. Chem.* **2008**, *120*, 9255 – 9257.

[12] a) R. D. Adams, O. S. Kwon, M. D. Smith, *Inorg. Chem.* **2001**, *40*, 5322 – 5323; b) R. D. Adams, O. S. Kwon, M. D. Smith, *Inorg. Chem.* **2002**, *41*, 5525 – 5529; c) J. F. Chai, H. P. Zhu, A. C. Stückl, H. W. Rosesky, J. Magull, A. Bencini, A. Caneschi, D. Gatteschi, *J. Am. Chem. Soc.* **2005**, *127*, 9201 – 9206; d) D. Y. Lu, J. S. K. Yu, T. S. Kuo, G. H. Lee, Y. Wang, Y. C. Tsai, *Angew. Chem. Int. Ed.* **2011**, *50*, 7611 – 7615; *Angew. Chem.* **2011**, *123*, 7753 – 7757; e) L. Fohlmeister, S. Liu, C. Schulten, B. Moubaraki, A. Stasch, J. D. Cashion, K. S. Murray, L. Gagliardi, C. Jones, *Angew. Chem. Int. Ed.* **2012**, *51*, 8294 – 8298; *Angew. Chem.* **2012**, *124*, 8419 – 8423.

[13] a) A. R. Fout, F. Basuli, H. J. Fan, J. Tomaszewski, J. C. Huffman, M.-H. Baik, D. J. Mindiola, *Angew. Chem. Int. Ed.* **2006**, *45*, 3291 – 3295; *Angew. Chem.* **2006**, *118*, 3369 – 3373; b) G. L. Jiao, X. Y. Li, H. J. Sun, X. F. Xu, *J. Organomet. Chem.* **2007**, *692*, 4251 – 4258; c) C. Jones, C. Schulten, R. P. Rose, A. Stasch, S. Aldridge, W. D. Woodul, K. S. Murray, B. Moubaraki, M. Brynda, G. L. Macchia, L. Gagliardi, *Angew. Chem. Int. Ed.* **2009**, *48*, 7406 – 7410; *Angew. Chem.* **2009**, *121*, 7542 – 7546.

[14] a) C. Jones, C. Schulten, L. Fohlmeister, A. Stasch, K. S. Murray, B. Moubaraki, S. Kohl, M. Z. Ertem, L. Gagliardi, C. J. Cramer, *Chem. Eur. J.* **2011**, *17*, 1294 – 1303; b) Q. S. Dong, X. J. Yang, S. D. Gong, Q. Luo, Q. S. Li, J. H. Su, Y. X. Zhao, B. Wu, *Chem. Eur. J.* **2013**, *19*, 15240 – 15247.

[15] L. Pauling, *The Nature of the Chemical Bond*, 3rd ed., Cornell Univ. Press, New York, **1960**, chap. 7.

[16] a) O. Delgado-Friedrichs, M. O'Keeffe, O. M. Yaghi, *Acta Crystallogr. Sect. A* **2006**, *62*, 350 – 355; b) D. W. Feng, H. L. Jiang, Y. P. Chen, Z. Y. Gu, Z. W. Wei, H. C. Zhou, *Inorg. Chem.* **2013**, *52*, 12661 – 12667; c) D. W. Feng, Z. Y. Gu, J. R. Li, H. L. Jiang, Z. W. Wei, H. C. Zhou, *Angew. Chem. Int. Ed.* **2012**, *51*, 10307 – 10310; *Angew. Chem.* **2012**, *124*, 10453 – 10456; d) Z. Chang, D. S. Zhang, T. L. Hu, X. H. Bu, *Cryst. Growth Des.* **2011**, *11*, 2050 – 2053; e) X. L. Zhao, X. Y. Wang, S. N. Wang, J. M. Dou, P. P. Cui, Z. Chen, D. Sun, X. P. Wang, D. F. Sun, *Cryst. Growth Des.* **2012**, *12*, 2736 – 2739.

[17] A. L. Spek, *J. Appl. Crystallogr.* **2003**, *36*, 7 – 13.

[18] a) M. C. Biesinger, B. P. Payne, A. P. Grosvenor, L. W. M. Lau, A. R. Gerson, R. St. C. Smart, *Appl. Surf. Sci.* **2011**, *257*, 2717 – 2730; b) M. Toupin, T. Brousse, D. Bélanger, *Chem. Mater.* **2004**, *16*, 3184 – 3190; c) C. S. Fadley, D. A. Shirley, A. J. Freeman, P. S. Bagus, J. V. Mallow, *Phys. Rev. Lett.* **1969**, *23*, 1397 – 1401; d) J. C. Carver, G. K. Schweitzer, T. A. Carlson, *J. Chem. Phys.* **1972**, *57*, 973 – 982; e) K. Okada, A. Kotani, *J. Phys. Soc. Jpn.* **1992**, *61*, 4619 – 4637; f) H. W. Nesbitt, D. Banerjee, *Am. Mineral.* **1998**, *83*, 305 – 315.

[19] a) Y. Gorlin, T. F. Jaramillo, *J. Am. Chem. Soc.* **2010**, *132*, 13612 – 13614; b) C. Bosch-Navarro, E. Coronado, C. Martí-Gastaldo, B. Rodríguez-González, L. M. Liz-Marzán, *Adv. Funct. Mater.* **2012**, *22*, 979 – 988; c) M. Chigane, M. Ishikawa, *J. Electrochem. Soc.* **2000**, *147*, 2246 – 2251; d) L. F. Chen, Z. H. Huang, H. W. Liang, Q. F. Guan, S. H. Yu, *Adv. Mater.* **2013**, *25*, 4746 – 4752.

[20] W. T. Liu, H. H. Thorp, *Inorg. Chem.* **1993**, *32*, 4102 – 4105.

[21] a) Q. X. Jia, H. Tian, J. Y. Zhang, E. Q. Gao, *Chem. Eur. J.* **2011**, *17*, 1040 – 1051; b) A. Shapiro, C. P. Landee, M. M. Turnbull, J. Jornet, M. Deumal, J. J. Novoa, M. A. Robb, W. Lewis, *J. Am. Chem. Soc.* **2007**, *129*, 952 – 959.

[22] J. A. Mydosh, *Spin Glasses: An Experimental Introduction*, Taylor & Francis, London, **1993**.

Received: May 26, 2015
Revised: July 10, 2015
Published online: August 10, 2015

